Physics of the Solid State, 2022, Vol. 64, No. 3

03,13

Study of silicon-to-silicon carbide transformation stages in the process of atomic substitution by the methods of total external X-ray reflection and X-ray diffractometry

© *S.A. Kukushkin* [1], *A.V. Osipov* [1], *E.V. Osipova* [1], *V.M. Stozharov* [2]

[1] Institute of Problems of Mechanical Engineering, Russian Academy of Sciences,
St. Petersburg, Russia
[2] Scientific and Technical Center „New Technologies“,
St. Petersburg, Russia
E-mail: sergey.a.kukushkin@gmail.com

Received November 3, 2021
Revised November 3, 2021
Accepted November 4, 2021

X-ray diffraction and total external reflection of X-rays (X-ray reflectometry) methods were used to study the successive stages of synthesis of epitaxial SiC films on Si (100) X-ray diffraction and total external X-ray reflection (XRD) methods were used to study successive stages of synthesis of epitaxial SiC films on Si (100) surfaces, (110) and (111) surfaces by the atom substitution method. The data on the transformation evolution of (100) surfaces were studied, (110) and (111) Si, into SiC surfaces. A comparative analysis of the X-ray structural quality of the SiC layers grown on Si by the atom substitution method with the quality of SiC layers grown by Advanced Epi by the standard CVD method. A modified technique for the total outer X-ray reflection method, based on measurements of the intensity of the reflected X-rays using a special parabolic mirror. It is shown that the method of total external reflection method makes it possible to obtain important information about the degree of surface roughness of SiC layers, the evolution of their crystal structure and plasmon energy in the process of Si to SiC conversion.

Keywords: total external reflection, X-ray reflectometry, silicon carbide, plasmons.

DOI: 10.21883/PSS.2022.03.53187.232

1. Introduction

The phenomenon of total external reflection of X-rays (TER), in which X-rays do not enter the second medium and are almost completely reflected at the interface between media with different refractive indices [1–5], is observed at glancing angles smaller than a certain critical ones α_c. If an X-ray beam is incident on the interface between media and its angle of incidence is less than α_c, then the X-rays are specularly reflected, penetrating in the process at $1-2$ nm deep into the substance. The limiting angle (critical angle) α_c is extremely small and depends on the electron density of the material. The higher the angle of the incident X-ray beam with respect to the limiting angle, the greater the depth of X-ray penetration into the material. For materials whose surface can be considered ideally flat, the reflectivity decreases sharply at angles greater than the limiting one. The increase in the surface roughness of the material leads to the sharp decrease in the reflectivity of this surface. If the material having a flat surface is used as a substrate and uniformly coated with the layer of another material whose electron density differs from the electron density of the initial surface, then X-rays will interfere with each other when reflected from the surface of a thin film and from the interface between the substrate and the film, forming an oscillatory pattern. In the first approximation, the intensity of the rays scattered by the sample is proportional to the square of the Fourier transform modulus of the electron density [1–5]. Thus, the electron density profile can be calculated from the measured X-ray intensity, and then the layer thicknesses, their roughness, and the number of other properties can be determined. In particular, the film thickness can be determined from the analysis of the oscillation periodicity (by analogy with ellipsometry), but information about the surface and interphase boundaries of the films can be found from the angular dependence of the oscillation amplitude. The reflectometry method [1–5] is based on these measurements. Recently, the X-ray reflectometry method has been widely used to determine the thickness, density, and roughness of both single-layer and multilayer film structures [2]. The advantages of X-ray reflectometry are that it allows to determine: the roughness of surfaces and interfaces between media (typical size of inhomogeneities is less than 5 nm), the thickness of the material layer (usually for layers thinner than 200 nm), the electron density distribution and internal constitution of complex structures [2].

According to the classical theory of X-ray diffraction [6,7], the refractive index n of X-rays in any solid is less than unity. Moreover, in the X-ray region of the spectrum of electromagnetic radiation, the refractive index is related to

the decrement of the refractive index $\delta = 1 - n$, which is directly proportional to the volume density of atoms N_{aV} [6,7]:

$$\delta = \frac{\lambda^2 e^2}{2\pi mc^2} N_{aV} f(0), \qquad (1)$$

where $\lambda = 1.5406$Å is X-ray wavelength $\mathrm{Cu}_{\mathrm{K}\alpha1}$; e is the electron charge; m is the electron mass; c is the speed of light; $f(0)$ is the atomic scattering factor in the direction of the incident X-ray radiation (for monatomic substance, the atomic factor is equal to the ordinal number of the element Z). Please note, that this definition of the refractive index is not entirely correct [8]. Strictly speaking, this definition is based on the assumption that the electromagnetic wave length is $\lambda \gg a$, where a is the interatomic distance. Formula (1) is obtained from the condition of the connection of the electric induction vector with the electric field strength vector using the dielectric constant. According to [8], the expression (1) can be used only if the X-ray frequency ω is much greater than the electron rotation frequency in the atom ω_0, i.e. $\omega \gg \omega_0$. This condition, as a rule, is satisfied for the outer electron shells in atoms, but it may not be satisfied for the inner electron shells of heavy atoms. If this is the case, then one should take into account the fact that the usual definition of dielectric constant, as a coefficient relating electrical induction to electric field strength, is not complete. Only external electrons contribute to the usual dielectric constant. The contribution of internal electrons is calculated by averaging over the entire volume of electron shells, and the permittivity and, accordingly, the refraction index become dependent on spatial coordinates $\mathbf{r}$ [2,8]. For small values of the difference between the wave vectors of the incident and scattered radiation, the electron density $n_e(\mathbf{r})$ reduces to the averaged electron density $\bar{n}_e$ [2,8]. In this case, when X-rays pass through the crystal, their refraction occurs, in full accordance with the laws of geometric optics. However, it should be remembered that the roughness will lead to X-ray diffraction in thin surface layers. Obviously, the radiation resulting from diffraction and the radiation resulting from reflection can be superimposed on each other.

The position of the maximum on reflection curves at small (close to zero) grazing angles α uniquely determines the X-ray refractive index and, as shown in [2,9], is related to it by the simple relationship

$$n = \cos\alpha. \qquad (2)$$

If the surface of the sample is rough, then part of the radiation is not reflected in the specular direction, but is scattered at other angles. The so-called diffuse reflection is formed. In this case, the intensity of the specular reflection decreases. The degree of specular reflection reduction is determined by the features of the surface relief pattern. This phenomenon has been studied in detail in works [1–5].

By measuring the decrement of the refraction index δ, by formula (1) one can determine the density of electrons per unit volume $n_e = N_{aV} f(0)$. Since the density of atoms is $N_{aV} = N_A \rho/\mu$, where N_A is the Avogadro's constant, ρ is the density of matter, μ is the molecular weight, then the value δ can be used to determine the mass density ρ of the substance under study. The presence of some transition layer of variable composition is determined by the nature of the decay of the scattering curve. However, this requires the use of special mathematical models and specialized computer programs [2,7]. The method of X-ray reflectometry can be implemented on an X-ray diffractometer, which makes it possible to carry out measurements in the region of small angles of incidence of an X-ray beam on the sample. The TER method is currently being intensively developed. This method is widely used in the study of thin films of various substances, Langmuir–Blodgett films, various adsorbed layers. All the possibilities of analyzing the structure of substance by this method have not yet been fully elucidated [2]. One thing is clear — the TER method is very promising as the method for analyzing the fine structure of surface layers of crystals of various nature. In particular, it turned out that if a plane X-ray wave with the wave vector $\mathbf{k}_0$ is incident on a crystal and for some reciprocal lattice vector of the crystal $\mathbf{h}$ the Wulf–Bragg condition condition is fulfilled $(\mathbf{k}_0 + \mathbf{h})^2 = k_0^2$, then the amplitude of the scattered X-ray wave in the crystal becomes comparable to the amplitude of the refracted wave [4]. In this case, the intensity of the wave field becomes dependent on the direction of the reciprocal lattice vector [4]. Moreover, this dependence is periodic, and the period of the standing wave is either exactly equal to or the integer number of times less than the interplanar distance d for the considered system of reflecting planes $|\mathbf{h}| = 2\pi n/d$ [4]. In this case, the field intensity is the same on planes parallel to the reflecting planes of the crystal. The so-called dynamic diffraction appears. The slightest disturbances in the crystal structure lead to the destruction of the periodicity and make it possible to observe the slightest changes in the crystal structure [2,4]. The practical use of this technique is associated with the observation of X-ray photo- and Auger electrons, which requires special precision equipment. However, as will be shown below, it is possible to obtain important data on the structure of matter using only the slightly modified TER method. In works [9–12] the technique for X-ray TER analysis was developed, based on measuring the intensity of reflected X-rays during grazing incidence of a paraxial beam with the grazing angle of about $0.5'$. The paraxial beam was formed using special parabolic mirror. This technique makes it possible to record a TER X-ray diffraction pattern in the $2\theta-\theta$ mode and construct the differential TER curve, on which the TER maximum [9] is clearly distinguished. At the same time, it turns out that the angular position of this maximum characterizes the refraction index of X-rays and the associated information about the surface structure of the crystal.

The characteristic feature of X-ray TER is that it essentially depends on which crystallographic planes lying near the surface of crystallites are parallel to the surface of these crystallites [10].

The purpose of this work is to study the surface structure features of silicon carbide (SiC) films grown on silicon (Si) by the method of matched substitution of atoms [13] by the modified TER method using a parabolic mirror under various conditions. The work will also compare SiC films grown on Si by atomic substitution [13,14] with SiC films grown by chemical vapor deposition (CVD) by Advanced Epi (https://advancedepi.com /sic/).

2. Features of the surface structure of SiC on Si samples grown by the method of matched substitution of atoms, and the conditions for their synthesis for study by the TER method

It follows from the results of works on the synthesis of SiC by the method of matched substitution of atoms, generalized in reviews [13,14], that the surface roughness of SiC/Si samples undergoes significant changes during the synthesis of SiC films. In [14] there are *in situ* plots of the change in the reflection of a light beam of a semiconductor laser with a wavelength of 650 nm from the surface of a silicon substrate undergoing transformation into SiC. As a result of the research, it was found that at different time stages of synthesis, the surface roughness of both the initial Si substrate and the SiC film undergo significant changes. It turned out [14] that the strongest changes in the surface structure occur in the first minutes (from 1 to 5 min) of the growth of the SiC layer. With longer synthesis times, the SiC surface becomes smooth [14]. The reasons for the change in roughness are related to the features of the formation of SiC layers. In the process of replacing Si atoms with C atoms, the chemical transformation of Si into SiC occurs with the simultaneous phase transition, the formation of pores in Si under the SiC layer and shrinkage pores in the surface layers of SiC. Detailed presentation of all ongoing processes, their theoretical analysis and experimental studies can be found in [13,14]. In [13–15] the reasons for the significant difference in the mechanisms and rates of transformation of Si into SiC on the Si (111) and Si (100) surfaces were explained.

The transformation of Si into SiC occurs as the result of interaction of carbon monoxide (CO) with crystalline silicon [13–16]. The distinctive feature of the method of matched substitution of atoms is that, regardless of the initial Si crystallographic plane on which SiC was synthesized, the (111) plane is necessarily formed as one of the planes. This effect is due to the fact that carbon-vacancy structures are always located along the $\langle 111 \rangle$ direction and lie in the $(\bar{1}10)$ plane perpendicular to the (111) plane. According to [14], at the initial stage of transformation of Si into SiC, the (100) Si face turns into a SiC face consisting of many facets resembling sawtooth structures, the side faces of which are covered with planes (111) and (110) and (210). At elevated CO pressures, the thin even SiC film is formed on the surface of the (100) Si face very quickly, much faster than on the (111) face. It should be noted, that the consistent quantum-chemical model for the growth of SiC on Si by the method of matched substitution of atoms was presented in the work [16].

To analyze the formation of the roughness of SiC layers from the time of synthesis, several SiC samples were synthesized. The samples were grown on the surface of (111), (100), and (110) Si faces at the following synthesis times: 1, 4, 12, 40 min. The synthesis temperature for all samples was 1270°C. The CO gas pressure during growth was maintained at $P_{\mathrm{CO}} = 67$ Pa. For the purity of the experiment, gaseous silane (SiH_4), which is usually added to the main CO gas in the synthesis of SiC [13,14], was not used. For comparison, we examined SiC samples grown on Si using the standard CVD method by Advanced Epi (https://advancedepi.com/sic/). It should be noted that SiC films grown on Si by the atom substitution method were studied in the works [17,18] using the X-ray reflectometry method. In these works, it was found that SiC films consist of a number of layers parallel to the substrate, resembling a „puff pastry pie“ with the composition varying from the surface towards the Si substrate. However, the evolution of roughness was not studied in these works, and the technique for measuring the TER was different [17,18].

3. TER measurement procedure

Studies of the properties of single crystal Si and epitaxial films of silicon carbide on the Si surface were carried out on a DRON-7 X-ray diffractometer with the copper anode and the parabolic mirror between the X-ray tube

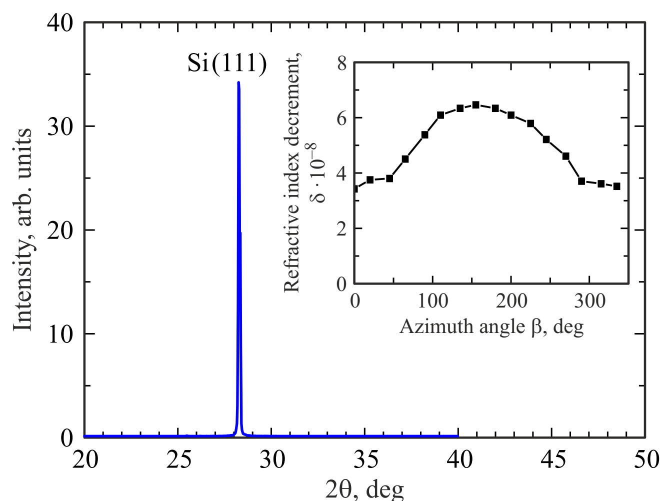

Figure 1. X-ray diffraction pattern in the (111) plane of a Si single crystal. The inset shows the dependence of the decrement of the refraction index δ on the sample rotation angle.

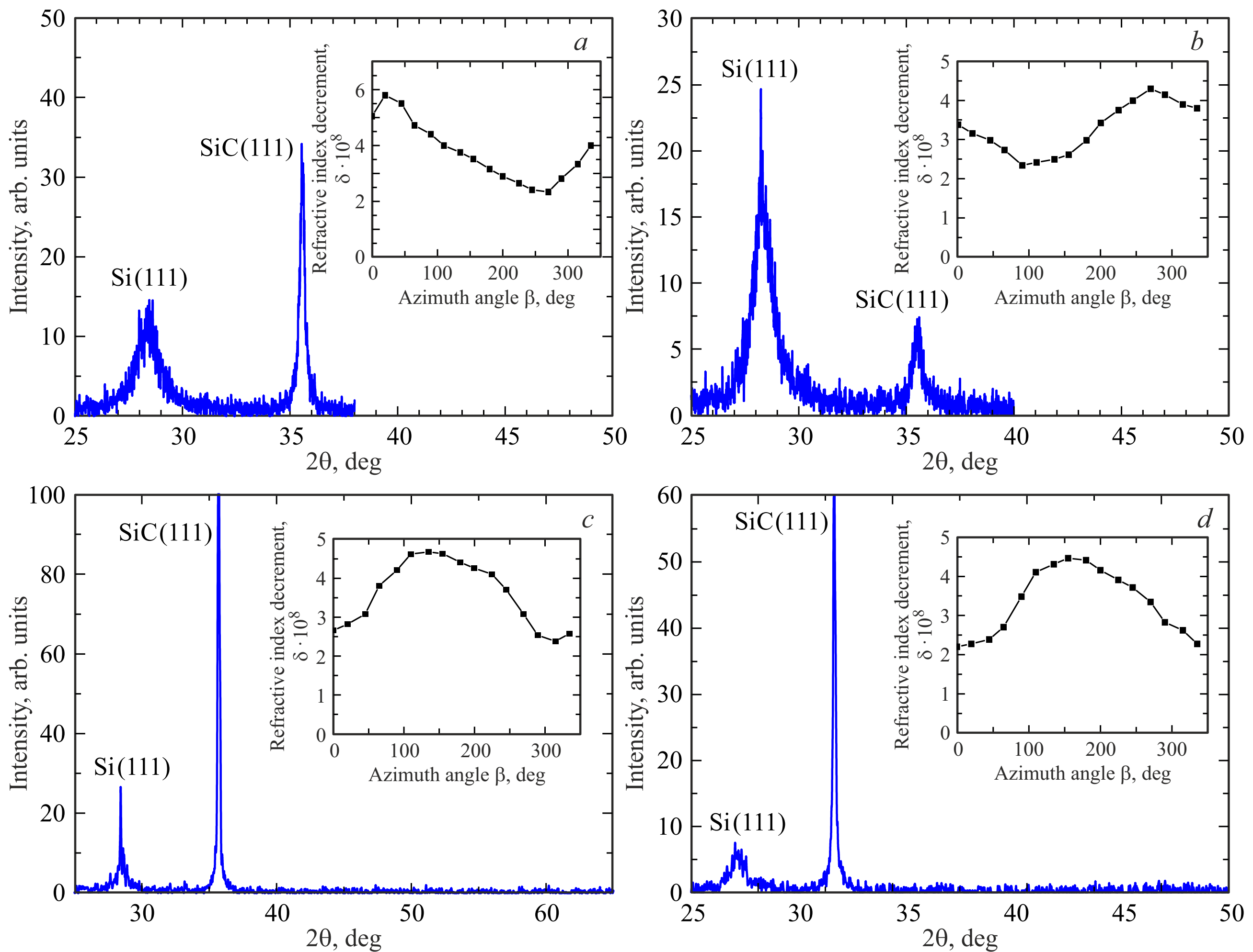

Figure 2. X-ray diffraction patterns of SiC samples grown at different synthesis times on Si (111). Synthesis times (*a*) — 1 min; (*b*) — 4 min; (*c*) — 12 min; (*d*) — 40 min; the temperature of synthesis of all samples was 1250°C, gas pressure — CO $P_{CO} = 67$ Pa. The insets show the dependences of the decrement of the refractive index δ on the rotation angle for these samples.

window and with the sample, which ensures the formation of the paraxial X-ray beam with the divergence of less than the arc minute and suppression parasitic spectral line CuK_β. The use of software made it possible to separate the $CuK_{\alpha 1}/CuK_{\alpha 2}$ spectral doublet and carry out all measurements on monochromatic $CuK_{\alpha 1}$ X-rays with the wavelength of $\lambda = 1.5406$ Å, which corresponds to the X-ray quantum energy $E = 8048$ eV. The use of the parabolic mirror in combination with the „$2\theta - \theta$" measurement mode and the collimator in front of the detector made it possible to record the differential total external reflection of X-rays. The projection area of narrow X-ray beam onto the sample surface is 1.6 cm^2. As a standard TER spectrum, the TER spectrum was taken from the (111) Si surface. Figure 1 shows the X-ray diffraction pattern of the initial Si sample and the decrement of the refraction index as the function of the azimuth rotation angle β.

Please note that the diffraction pattern shown in Fig. 1 corresponds to single-crystal silicon of the cubic system with the crystal lattice constant of $a = 5.465$ Å. The starting point in the construction of the TER was determined as follows. To construct the TER of Si (111) orientation, the diffraction pattern was first taken (see Fig. 1) and the maximum of the diffraction peak corresponding to the (111) Si plane was chosen as the reference point, i.e. the angle $2\theta = 28.26°$, in which the maximum X-ray diffraction intensity is observed. Then the sample was rotated by the azimuth angle β, which varied from 0° to 357° counterclockwise with the step of $\Delta\beta = 21°$. Every 21° the angle at which TER is observed was determined. The TER from SiC films was taken similarly, only the maximum of the diffraction peak corresponding to the (111) SiC plane was taken as the reference point. If for any Si sample with SiC the intensity of the SiC peak was less than the intensity of the Si peak, then the counting started from the Si peak. This angle differed slightly for each of the samples, since strains in the SiC film lead to a shift of the diffraction peak with respect to the table data of the diffraction peak of this plane of unstressed cubic SiC. In this case, the glancing

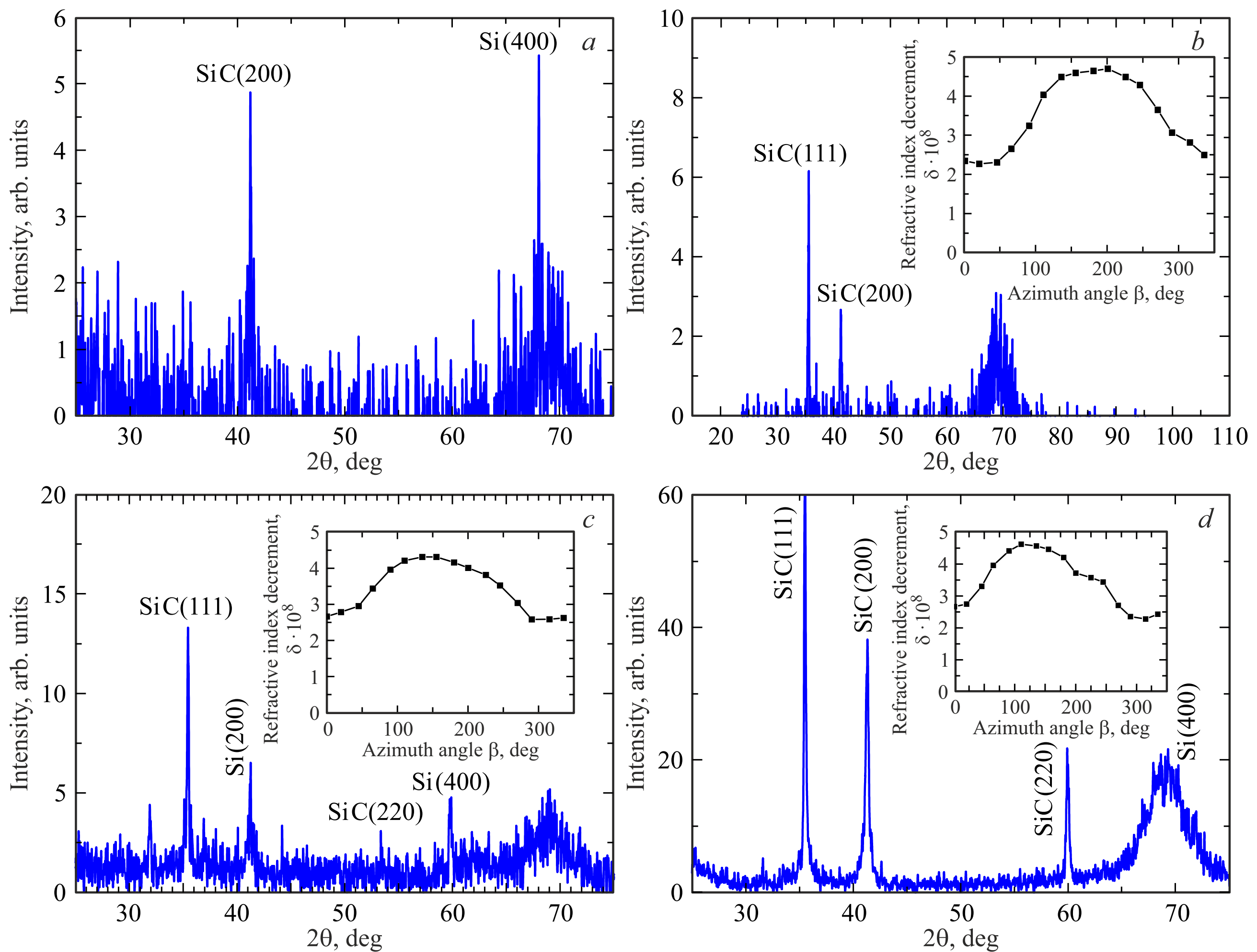

Figure 3. X-ray diffraction patterns of SiC samples grown at different synthesis times on Si (100). Synthesis times (*a*) — 1 min; (*b*) — 4 min; (*c*) — 12 min; (*d*) — 40 min; the temperature of synthesis of all samples was 1250°C, gas pressure — CO $P_{CO} = 67$ Pa. SiH_4 was absent during synthesis. The insets show the dependences of the decrement of the refractive index δ on the rotation angle for these samples.

angles α were determined. Based on the values of these angles, the dependence of the decrement of the refractive index δ on the angle of rotation of the sample was plotted. It should be noted, that, as a rule, silicon is covered with thin layer of oxide. Therefore, the dependence δ shown in Fig. 1 may be due to the influence of silicon oxide and the Si-oxide interface on the TER. In the general case, the special formulation of studies of this structure is needed. It should be noted that SiC does not oxidize in air at room temperature, so we can assume that there are no oxides on its surface. The surface of SiC samples grown on Si (100) by the method [13,14], as shown in [15], is mainly covered with (111) faces, in contrast to SiC films grown on standard procedure [13], whose surface is covered with (100) faces. To determine the point of reference for the TER of the SiC layer grown by the method [13,14] on Si (100), we used the diffraction peak from the (200) plane, since, as will be seen below, only this SiC peak appears on film of this orientation.

4. Experimental results

Figure 2 shows the diffraction patterns and dependences of the refractive index decrement δ on the sample rotation angle for SiC samples grown at different synthesis times on Si (111). The synthesis temperature for all samples was 1250°C, and the CO gas pressure was $P_{CO} = 67$ Pa. SiH_4 was absent during synthesis.

Figure 3 shows the diffraction patterns and dependences of the refraction index decrement δ on the rotation angle for SiC samples grown at different synthesis times on Si (100). SiC samples on Si (111) and Si (100) were grown in the same process.

To compare the TER spectra of SiC samples grown by the matched atomic substitution method with SiC samples grown by the standard procedure, Fig. 4 shows X-ray diffraction patterns and dependences of the refractive index decrement δ on the rotation angle for SiC samples grown by the CVD method (https://advancedepi.com/sic/). SiC films

grown on three different surfaces of Si substrates, namely, on Si (111), on a vicinal Si (111) surface deviated by 4°, and on a Si (100) surface, were investigated.

5. Discussion of results

The X-ray patterns shown in Figs. 2 and 3 clearly show the change in time of the crystal structure of Si in the process of its transformation into SiC by the method of coordinated substitution of Si atoms for C atoms. The evolution of the structure is especially well seen in the example of SiC films synthesized on the (100) Si surface (Fig. 3).

In the first minute of synthesis, the reflection appears on the (111) Si surface, corresponding to the (111) SiC plane, and the curve of dependence of the decrement of the refraction index δ on the rotation angle has the form of broken line. On the (100) Si surface, silicon carbide has not yet formed during this time. Intense scattering of X-rays occurs. Silicon is in a state of transition to SiC. Only the (200) SiC planes in the second order of the Bragg diffraction and the (400) plane of silicon in its fourth order are determined with difficulty. The surface becomes very rough, for that reason we were unable to record the TER spectra from this surface. Previously, in a review [14] on the reflection of light from a surface, it was experimentally shown that approximately in the first hundred seconds of synthesis, silicon carbide itself is formed from an intermediate complex „silicon saturated with silicon vacancies and carbon atoms“, which in [13,14] are called as „dilatational dipoles“. This formation is accompanied by a sharp rearrangement of the silicon structure, its transformation into SiC with shrinkage, leading to the formation of pores and the development of surface roughness. The process of transformation of Si into SiC on the surface (100) going differently [15]. The structure is formed on the surface, which is „grooves“, the walls of which are covered with faces (facets) of SiC orientation (111). „The bottom of the grooves“, where the (111) faces meet, is a narrow section of the face with the (100) orientation. „Grooves“ are oriented along the $\langle\bar{1}10\rangle$ direction. That is why, during the growth of SiC, the complete rearrangement of the Si surface layer occurs first, and only then does the (111) face crystallize. Nothing similar is observed during the growth of SiC on Si by the standard procedure. During growth by the CVD method, as it should be, (100) faces are formed rather than (111) faces. This is clearly seen from the X-ray patterns shown in Fig. 4. However, since, as a rule, gaseous hydrocarbons (or vapors of carbon-containing alcohols) are used in the growth of SiC by the CVD method, in this case, too, Si atoms should be partially replaced by C atoms. Naturally, this process is different and more chaotic than the process using the substitution reaction [13]. The replacement will „overlay“ on the main growth process. In our opinion, this is precisely why the SiC layer on Si grown by the method (https://advancedepi.com/sic/) does not have high crystalline perfection, which is clearly seen in Fig. 4, *c*.

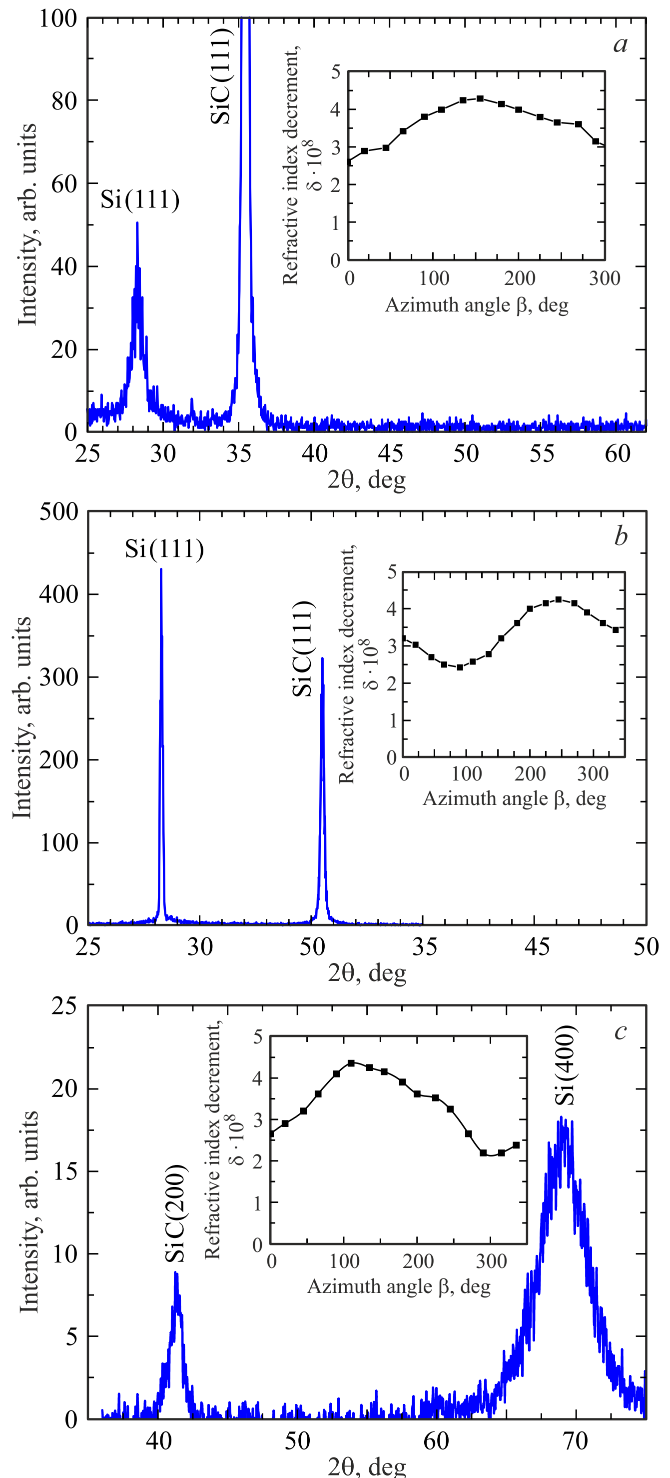

Figure 4. X-ray diffraction patterns of SiC samples grown by the CVD method (https://advancedepi.com/sic/) on Si of various orientations. (*a*) on Si (111); (*b*) on Si (111) with the deviation of 4°; (*c*) on Si (100). The insets show the dependences of the decrement of the refractive index δ on the angle of rotation of these samples.

It can be seen from the X-ray patterns shown in Fig. 3 that, at the synthesis time from 1 to 4 min, epitaxial SiC is formed on the surface of the (111) Si face. Already at 1 min of synthesis, the (111) Si face transforms into the (111) SiC face. The final formation of the SiC layer occurs between 12 and 40 minutes of synthesis. The Bragg diffraction angle shifts towards larger values, which indicates the decrease in strain. The shift of the peaks makes it possible to estimate the strains occurring in the SiC films. Deformations were evaluated as follows. First, the location of the main X-ray peaks of the first and second orders (if they were present) of the X-ray pattern on the 2θ axis was determined. Then, based on the angular positions of the lines and the Bragg equation, the values of the interplanar distances were calculated. These interplanar distances were calculated for both first and second order peaks. The calculated values of interplanar distances were compared with their tabular values for the 3*C*-SiC polytype. Then, relative strains were calculated for planes calculated from the peaks of X-ray reflections of the first and second orders. As a rule, they matched. If there was a difference between them, it was modest. If differences were observed, then their average value was used to estimate the strains. The calculations showed the following: in the SiC film synthesized for 1 min, tensile strain $\varepsilon_{111} = 3 \cdot 10^{-3}$ occurs; in a film synthesized for 4 min, the tensile strain takes on the value $\varepsilon_{111} = 2 \cdot 10^{-3}$; and in a film synthesized for 12 min, the tensile strain is replaced by a weak compressive strain $\varepsilon_{111} = -9 \cdot 10^{-4}$. In the future, the strain remains unchanged, fluctuating, depending on the experimental conditions, around zero. In a film synthesized for 40 min, a tensile strain again arises equal to $\varepsilon_{111} = 4 \cdot 10^{-4}$. Such changes can be considered an experimental error. We believe that after 12 min there are no strains in the film caused by both the difference in the lattice parameters and the difference in the coefficients of thermal expansion. This fully confirms the conclusion made in [14,16] about the fundamental difference between the mechanism of SiC growth by the method of coordinated substitution of atoms from the classical mechanism, in which tensile strains always occur during the growth of SiC on Si. Please note that the difference in the thermal expansion coefficients is leveled out during the growth of SiC by the method of coordinated substitution of atoms by the formation of pores under its surface [13,14].

Let us consider the growth of SiC on the (100) Si surface. In full accordance with the theory of growth described in the works [14,15], in this case only tensile strains occur. Their value is of the order of strain on the (111) surface Thus, for growth times 1–4 min, the strains are $\varepsilon_{100} = 3 \cdot 10^{-3}$ and $\varepsilon_{111} = 3 \cdot 10^{-3}$, respectively. At growth times 12–40 min, the strains decrease somewhat and remain at the level of $\varepsilon_{100} = 5 \cdot 10^{-3}$ and $\varepsilon_{111} = 5 \cdot 10^{-3}$ at 12 min growth and $\varepsilon_{100} = 3 \cdot 10^{-3}$ and $\varepsilon_{111} = 5 \cdot 10^{-3}$ for 40 min of growth, respectively.

Let us consider the diffraction patterns of SiC samples grown on Si by the CVD method by Advanced Epi

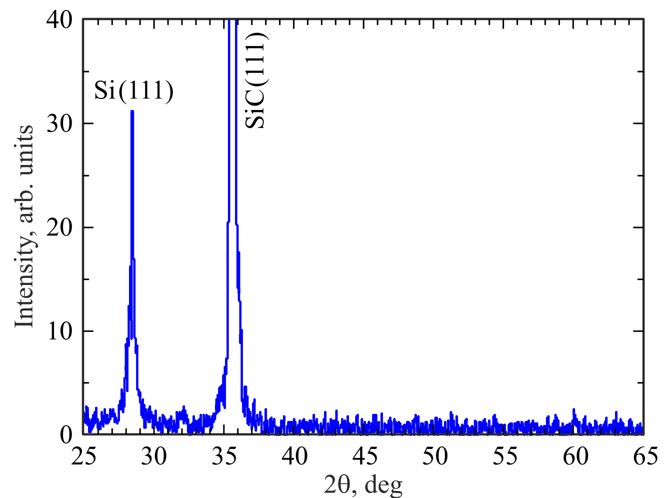

Figure 5. X-ray diffraction pattern of a SiC sample on Si synthesized from a mixture of CO and SiH_4 gases. Synthesis temperature is 1290°C, total gas mixture pressure is $P = 307$ Pa, CO flux is 12 cm^3/min, SiH{4} flux is equal to 4 cm^3/min, synthesis time is 15 min.

(https://advancedepi.com/sic/) (Fig. 4). The SiC sample grown on (100) Si is practically not stressed. This is not surprising since the SiC layer is not an epitaxial film, but the texture. It can be seen from the X-ray diffraction pattern of this sample that it has only a second-order reflex from the (100) plane. In addition, this also follows from the data on electron diffraction (RHEED) not presented here. Because this sample is textured, its tensile strain is small and is of the approximately equal order $\varepsilon_{100} \sim 9 \cdot 10^{-5}$. The samples obtained on (111) and (111) with a deviation of 4° are stretched. The tensile strain of these samples is equal $\varepsilon_{111} = 5 \cdot 10^{-3}$.

It should be noted, that the X-ray data shown in Fig. 2 and Fig. 3 are given only for SiC samples grown in pure CO. It was shown in works [14,16,19] and in the patent [20] that in order to obtain an epitaxial film of a high degree of crystalline perfection, gaseous monosilane (SiH_4) must be added to CO gas in a small proportion. The silane is needed to prevent excessive silicon evaporation and „healing" of shrinkage pores formed during the transformation of Si into SiC. We will present a study of the time dependences of the transformation, similar to those carried out in this work, in a separate study, and in this work we present only one X-ray diffraction pattern from a SiC layer grown from a mixture of CO and SiH_4 gases. This diffraction pattern is shown in Fig. 5.

The diffraction pattern completely lacks any SiC reflections except for the main (111) SiC reflection. This indicates the high quality of the SiC layer. In this case, the SiC layer is compressed. Compression strain is of the order $\varepsilon_{111} \sim -1 \cdot 10^{-3}$. If we take into account that the Young's modulus of the SiC film is equal to $E = 328$ GPa [21], and the Poisson's ratio is about $\nu \sim 0.45$, then under such

a deformation, the elastic compressive stresses reach the value of the order $\sigma \sim -0.6$ GPa. Thus, by changing the temperature, the pressure of the gas mixture, and the gas flow rate, it is possible to control the elastic stresses by changing their sign and magnitude. It should be noted, that the samples obtained by the CVD method are always stretched, and during the growth of SiC by the atom substitution method, both stretched and compressed SiC layers can be obtained. The explanation of this phenomenon is given in the works [13,14,19].

On the sample grown at a synthesis time of 4 min, the dependence curve of the decrement of the refraction index δ on the rotation angle, as well as for the sample grown at 1 min, has the form of broken line, but its maximum value lies in the opposite direction. At synthesis time of 12 min, the dependence of the refractive index decrement δ on the rotation angle becomes similar to analogous curve of pure silicon (see Fig. 1). In our opinion, this indicates the completion of the formation of the SiC epitaxial layer. On SiC films grown on (100) Si, the dependences of the decrement of the refractive index quickly acquire the complete form. The dependences of the refraction index decrement for samples obtained by the CVD method (https://advancedepi.com/sic/) have the similar form, except for the sample grown on the vicinal Si plane deviated by 4° from the (111) plane. The curve of this dependence is similar to the refraction index decrement for a SiC sample synthesized for 4 min (see Fig. 2, *b*). It should be noted, that the angular dependence of the refraction index decrement of the SiC film grown by the method of matched substitution of atoms on the vicinal surface of the Si substrate deviated by 4° from the (111) plane has a similar form (see Fig. 6, *a*). This type of dependence of the refractive index decrement for the vicinal surface on the angle of rotation of the plate is associated, in our opinion, with the scattering of light by SiC steps. The planes of these steps are perpendicular to the direction having the $[\bar{1}\bar{1}2]$ orientation. This orientation is perpendicular to the (111) plane. During the rotation of the crystal with the film, the maximum of the δ index will be observed at the moment when the glancing X-ray beam is perpendicular to the step plane, i.e. to direction $[\bar{1}\bar{1}2]$. SiC films grown by CVD method on vicinal faces retain this step orientation. In the process of transformation of Si into SiC during growth by the method of coordinated substitution of atoms, Si steps „are etched" and covered with SiC faces, in particular, (311) faces [13]. However, in general, the original direction of the general array of steps $[\bar{1}\bar{1}2]$ is preserved in this case as well. This means that when the Si substrate with the SiC film is rotated by 270°, the TER angle increases, which leads to an increase in the refraction index decrement δ. This is clearly seen both on the film grown by the CVD method (Fig. 5) and on the SiC film grown by the atomic substitution method (Fig. 6, *a*). To confirm this, a SiC layer was grown on the Si (110) surface by the substitution method. The film synthesis temperature was 1290°C, CO gas pressure was $P_{\mathrm{CO}} = 67$ Pa. SiH_4 was absent during synthesis. The sample was grown for 30 min. Figure 6, *b* shows the X-ray diffraction pattern of this sample, and the inset to it shows the dependence of its refractive index decrement δ.

To elucidate the reasons for the influence of the plate curvature and its roughness on the X-ray characteristics, similar dependences of the refraction index decrement δ on the azimuth angle of rotation for the plate made of copper were plotted. Copper was chosen for two reasons. First, as silicon and as cubic polytype of silicon carbide, copper crystallizes into the cubic face-centered lattice (with the only difference that the SiC lattice is of the diamond type). Secondly, copper is a metal, not a semiconductor, so it is interesting to check whether the shapes of the TER curves for a metal and a semiconductor differ. According to the theory [6] and formula (1) this should not be observed. The initial copper plate, consisting of polycrystalline copper, was polished. The TER and XRD diffraction pattern was made from its surface. Then, deep grooves were applied to the surface of this plate in one direction. After that, the TER and XRD diffraction pattern was made from its surface. The dependences of the decrement δ for the copper plate are shown in Fig. 6, *c*. It follows from these data that decrement δ dependences for polished and rough surfaces differ from each other. The behavior of the decrement δ for the polished surface, as can be seen, is similar to the behavior of the decrement for the SiC layer grown on Si (111) and Si (100) at the final stage of its formation. On the rough surface of the copper plate, the dependence of the decrement δ on the azimuth angle resembles its behavior at the initial stages of SiC formation on (111) and on the (110) surface. This, as well as the behavior of the index δ for the (110) SiC surface, explains the behavior of the value on the SiC (111) surfaces too. Indeed, let us turn to Fig. 2, *a*. The maximum value of the decrement of the refraction index δ at 1 min of SiC layer growth takes on if the grazing X-ray beam is directed along the $\langle 1\bar{1}0\rangle$ direction. It reaches its minimum value when the sample is rotated by 270°. This means that it is along this direction the main changes in the structure of both Si and SiC occur in the first-ever minutes of synthesis. Actually, this also follows from the form of the diffraction pattern (Fig. 2, *a*), which was discussed above. The SiC diffraction peak is higher than the Si peak. In this case, both peaks are rather blurred, which indicates the restructuring of the structure. Obviously, along the $\langle 1\bar{1}0\rangle$ direction, a deflection of the plate occurs, which leads to an increase in the reflection angle. After three minutes of synthesis, the picture radically changes (Fig. 2, *b*). The refraction index decrement δ curve takes the form similar to the refraction index decrement δ for films grown on vicinal Si surfaces (Fig. 5 and Fig. 6). The X-ray spectrum changes too. The intensity of the peak from silicon increases, while the intensity of the (111) SiC peak decreases.

From the experimental value of the refraction index decrement δ and formula (1), one can estimate the volume density of scattering atoms N_{aV} in the TER exit zone [10].

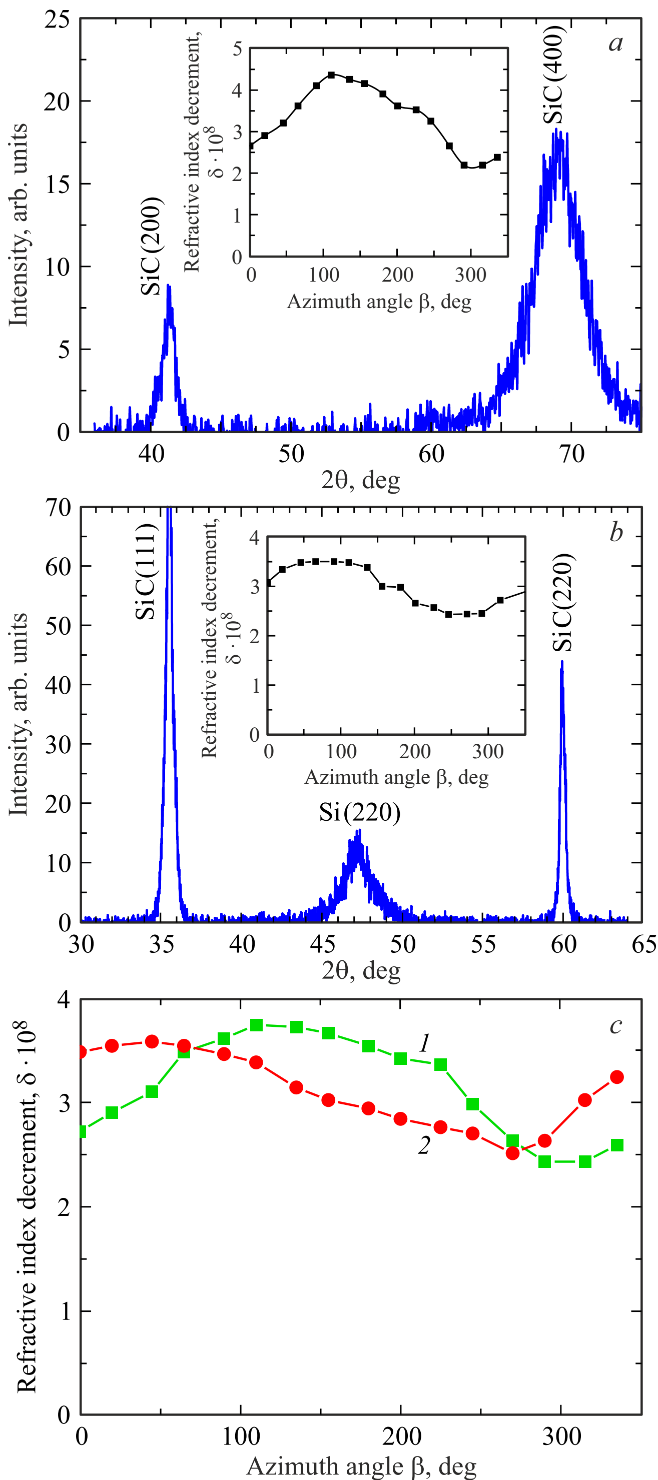

Figure 6. Dependences of the decrement of the refraction index δ on the rotation angle of various samples; (*a*) — a SiC sample grown by atomic substitution on Si (111) with a deviation of 4°; (*b*) — XRD diffraction pattern of the SiC/Si (110) sample and the dependence of its refraction index decrement δ (on the inset) on the rotation angle of the SiC sample grown on Si (110); (*c*) — dependence of the decrement of the refraction index δ on the angle of rotation of the copper plate; *1* — curve for the polished surface of the copper plate; *2* — curve for the copper plate with grooves applied to its surface.

Based on estimates of the value of N_{aV}, calculation of the depth of TER formation in a material, estimates of the range of an X-ray quantum in matter [22], one can estimate the density of localized electrons N_0 [23,24] involved in the formation of X-ray TER. Since plasma oscillations in solid state are excited not by X-ray quanta, but by slow secondary electrons generated by fast X-ray photoelectrons [25] in a thin surface layer λ thick, this thickness, with which the exit from the solid of slow electrons should be calculated using the Bronstein formula [26]:

$$\lambda = \frac{1.9 \cdot 10^{-7} \cdot A}{\rho \cdot Z^{0.6}}, \tag{3}$$

where A is the atomic mass; ρ is the density; Z is the sequential number of the element. It should be noted that plasma oscillations excited by X-rays are oscillations of bound electrons, according to [23] their frequency corresponds to high energy. These oscillations are not excited at thermal energies. According [23] the plasma oscillation energies cannot be identified with the optical gap between the top of the valence band and the bottom of the conduction band. This energy corresponds to the average distance between energy levels located vertically, one above the other in the reduced Brillouin zone [23].

Based on these data, one can estimate the density of electrons involved in the excitation of plasmons, and then estimate the energy of plasmons excited by X-rays during TER. More details about this procedure can be found in the works [7–10]. Above, based on the analysis carried out in [6], we noted that one should be careful when estimating the plasmon energy when using formula (1), since in the general case the refraction index may depend on spatial coordinates. It seems that this is exactly what is observed in the process of measuring the decrement δ during the rotation of the sample. Therefore, to estimate the plasmon energy for each of the SiC samples, we took only the minimum value δ, i.e., for each sample, only the minimum value of the TER angle was used, which is given in the insets to the corresponding X-ray patterns. Based on these values δ, the plasmon energies E_P were estimated. Thus, for Si the energy is $E_P = 2.11$ eV; for the SiC/Si (111) 4° layer — $E_P = 1.74$ eV; for the SiC/Si (111) layer synthesized for 1 min — $E_P = 1.74$ eV; for the SiC/Si (111) layer synthesized for 4 min — $E_P = 1.74$ eV; for the SiC/Si (111) layer synthesized for 40 min — $E_P = 1.74$ eV; for the SiC/Si (1100) layer — $E_P = 1.71$ eV. For samples grown by the CVD method, the values of E_P are as follows: for a SiC/Si (111) sample — $E_P = 1.85$ eV; for the SiC/Si (111) 4°sample — $E_P = 1.75$ eV; for the SiC/Si (100) sample — $E_P = 1.6$ eV. Once again, it should be noted, that the measured energies E_P cannot be identified with the optical band gap, although their values can be close, which is observed in this case, especially for SiC samples. We noted above that Si, as a rule, is covered with the oxide layer; therefore, the energy $E_P = 2.11$ eV may correspond not to pure Si, but to Si with an oxide layer. It follows from the

data that the energies E_P of the SiC layers obtained both by the CVD method and by the substitution method, but without the addition of silane, are close in value. When silane is added to CO gas during synthesis, the energy values E_P for the SiC layer increase. This, in our opinion, indicates the increase in the perfection of the crystal structure of the films. Thus, for the sample, whose X-ray spectrum is shown in Fig. 5, $E_P = 2.5$ eV. For comparison, the angular dependence of the decrement δ of the $4H$-SiC single crystal was measured by the TER method (due to the lack of space, these data are not presented here). The energy value E_P turned out to be equal to $E_P = 2.7$ eV, which is close to the value E_P for the SiC sample grown in the presence of silane. Thus, the energy value E_P can qualitatively indicate the presence or absence of defects in the crystal.

6. Conclusion

With the joint use of X-ray diffraction technique and X-ray TER methods to study the temporal stages of the synthesis of epitaxial SiC films on Si, data were obtained on the evolution of the transformation of the (100), (110) and (111) Si surfaces in the SiC surface in the process of coordinated substitution of a part of Si atoms by C atoms. It has been found that the final formation of the SiC layer at a temperature of $1250-1300^\circ$ is completed between 15 and 30 min of synthesis. The previously discovered [14,15] phenomenon of the formation of (111) faces as the main faces on the (100) and (110) Si surfaces using the atom substitution method is confirmed. On the example of samples manufactured by Advanced Epi (https://advancedepi.com/sic/), it is shown that when using the standard CVD growth method, the (100) SiC face is always formed on the surface of the (100) Si face. The previously discovered fact [13,14,16,19,20] of the significant improvement in the crystalline quality of the SiC layers and the change from tensile elastic strains in the SiC layer to compressive ones upon the addition of gaseous silane to gas CO was confirmed. It is shown that the experimental measurement of the decrement of the refractive index δ using TER provides important information on the evolution of the crystal structure during the transformation of Si into SiC.

Acknowledgments

The authors are grateful to Mr. V.K. Egorov for a useful discussion of a number of questions concerning X-ray TER.

Funding

The research was carried out as part of project № 20-12-00193 of the Russian Science Foundation.

The research was carried out using the equipment of the unique scientific facility „Physics, Chemistry and Mechanics of Crystals and Thin Films“ of Institute for Problems in Mechanical Engineering of the Russian Academy of Sciences, Federal State Unitary Enterprise (St. Petersburg).

Conflict of interest

The authors declare that they have no conflict of interest.

References

[1] P.F. Fewster Rep. Prog. Phys. **59**, 1339 (1996). DOI: 10.1088/0034-4885/59/11/001.

[2] M.A. Shcherbina, S.N. Chvalun, S.A. Ponomarenko, M.V. Kovalchuk. Uspekhi khimii. **83**, *12*, 1091 (2014) (in Russian). http://dx.doi.org/10.1070/RCR4485?locatt=label:RUSSIAN.

[3] V.E. Asadchikov, E.E. Andreev, A.V. Vinogradov, A.Yu. Karabekov, I.V. Kozhevnikov, Yu.S. Krivonosov, A.A. Postiov, S.I. Sagitov. Poverkhnost'. Rentgenovskie, sinkhrotronnye i nejtronnye issledovaniya. **7**, 17 (1998) (in Russian).

[4] M.V. Kovalchuk, V.G. Kon. Physics-Uspekhi **149**, 69 (1986).

[5] D.K.G. de Boer. Phys. Rev. B **51**, 5297 (1995).

[6] R. James. Optical Principles of the Diffraction of X-Rays. Ox Bow Pr (1982). ISBN-10: 0918024234.

[7] P. Chizhov, E. Levin, A. Mityaev, A. Timofeev. Pribory i metody rentgenovskoy difraktsii. Mozhaisk Printing and Publishing Integrated Works, Mozhaisk (2011). 151 p. (in Russian).

[8] L.D. Landau, E.M. Lifshitz. Teoreticheskaya fizika. Elektrodinamika sploshnykh sred. Nauka, M. (1992). V. VIII. 663 p. (in Russian).

[9] V.M. Stozharov. ZhTF, **87**, 125 (2017) (in Russian).

[10] V.M. Stozharov, V.P. Pronin. ZhTF, **87**, 1901 (2017) (in Russian).

[11] V.M. Stozharov. ZhTF, **89**, 1042 (2019) (in Russian).

[12] V.M. Stozharov. ZhTF, **90**, 1116 (2020) (in Russian).

[13] S.A. Kukushkin, A.V. Osipov, N.A. Feoktistov. FTT **56**, 1457 (2014) (in Russian).

[14] S.A. Kukushkin, A.V. Osipov. J. Phys. D **47**, 313001 (2014). DOI:10.1088/0022-3727/47/31/313001.

[15] S.A. Kukushkin, A.V. Osipov, I.P. Soshnikov. Rev. Adv. Mater. Sci. **52**, 29 (2017).

[16] S.A. Kukushkin, A.V. Osipov. J. Phys. D. **50**, 464006 (2017).

[17] S.A. Kukushkin, K.Kh. Nusupov, A.V. Osipov, N.B. Beisenkhanov, D.I. Bakranova. FTT **59**, 986 (2017) (in Russian).

[18] S.A. Kukushkin, K.Kh. Nussupov, A.V. Osipov, N.B. Beisenkhanov, D.I. Bakranova. Superlat. Microstruct. **111**, 899 (2017).

[19] S.A. Kukushkin, A.V. Osipov. Pis'ma v ZhTF **43**, 81 (2017) (in Russian). DOI: 10.21883/PSS.2022.03.53187.232

[20] S.G. Zhukov, S.A. Kukushkin, A.V. Lukyanov, A.V. Osipov, N.A. Feoktistov. Method for manufacturing products containing silicon substrate with the silicon carbide film on its surface. Patent № 2522812 RF dated May 21, 2014.

[21] A.S. Grashchenko, S.A. Kukushkin, A.V. Osipov. FTT **61**, 2313 (2019) (in Russian). DOI: 10.1134/S106378341912014X.

[22] M.V. Davidovich. Optika i spektroskopiya **126**, *3*, 360 (2019) (in Russian). DOI: 10.21883/PSS.2022.03.53187.232
[23] J. Ziman. Principles of solid-state theory (Printsipy teorii tverdogo tela). Mir, M. (1966). 315 p. (in Russian).
[24] P. Grosse. Free electrons in solids (Svobodnyye elektrony v tverdykh telakh). Mir, M. (1982). 470 p. (in Russian).
[25] V.A. Volkov. Plasmons and magnetoplasmons (Plazmony i magnitoplazmony). Institute of Radio Technologies and Electronics of the Russian Academy of Science, M. (2019). P. 1−7 (in Russian).
[26] I.M. Bronshtein, B.S. Fraiman. Secondary electron-emission (Vtorichnaya elektronnaya emissiya). Nauka, M. (1969). 174 p. (in Russian).